Supporting Information

A Multifunctional Nanoporous Carbon Platform Derived from Zeolitic Imidazolate Framework for Sensing and Enzyme-like Catalyst

Lin Lu,*[a] Xiaojing Li,[b] Junsong Mou,[c] Xiyue Cao,[c] and Jianfei Xia *[c]

[a.] Zibo Normal College, Zibo, Shandong, PR China.

[b.] Department of Oral Implantology, The Affiliated Hospital of Qingdao University, Qingdao, PR China

[c.] College of Chemistry and Chemical Engineering, Qingdao Application Technology Innovation Center of Photoelectric Biosensing for Clinical Diagnosis and Treatment, Instrumental Analysis Center of Qingdao University, Qingdao University, Qingdao, PR China.

* Corresponding author.

E-mail: xiajianfei@126.com

Fax: +86-532-85953280; Tel: 86-532-85953280

Contents

Chemicals and Materials

Zinc nitrate hexahydrate ($Zn(NO_3)_2 \cdot 6H_2O$, 99%) and hydroquinone ($C_6H_6O_2$, ≥99.0%, AR) were ordered from Aladdin Reagent Co., Ltd (Shanghai, China). 2-Methylimidazole ($C_4H_6N_2$, 98%) was ordered from Shanghai Macklin Biochemical Co., Ltd (Shanghai, China). Catechol ($C_6H_6O_2$, ≥98.0%, AR), ethanol (C_2H_5OH, ≥99.5%), potassium hydroxide (KOH), hydrogen peroxide (H_2O_2, 30%) were purchased from Sinopharm Chemical Reagent Co., Ltd (Shanghai, China). 3, 3', 5, 5'-Tetramethylbenzidine (TMB, $C_{16}H_{20}N_2$) was ordered from Sangon Biotech (Shanghai) Co., Ltd (Shanghai, China). Nafion solution (5%, DuPont) was diluted into 0.5 wt%. N, N-dimethylformamide, Na_2HPO_4, NaH_2PO_4, and other reagents were of analytical grade. The water used in this work was deionized water.

Apparatus and Characterization

Transmission electron microscopy (TEM) characterization were performed on JEOL JEM-1200. The surface topography was characterized by using field emission scanning electron microscopy (FESEM, Regulus 8100 Hitachi). Atomic force microscopy (AFM) images were collected by Bruker Multimode 8. X-ray diffraction (XRD) data was obtained by Rigaku D-MAX 2500/PC. The Raman spectra were recorded on Thermo Fisher Scientific Raman Microscope (DXR2) at an excitation wavelength of 532 nm at room temperature. Fourier Transform Infrared Spectrometer (FT-IR, Nicolet™ iS50 FTIR, United States) was used to study the surface groups of the obtained sample. The UV-vis spectra were performed with the UV-vis spectrophotometer (Shimadzu UV-2500, Japan). The fluorescence intensity of GQDs solution was recorded on an F-7000 fluorescence spectrometer (Hitachi, Japan). The electrochemical data were measured by PARSTAT 6000A electrochemical workstation with a traditional three-electrode cell (Princeton Applied Research, United States).

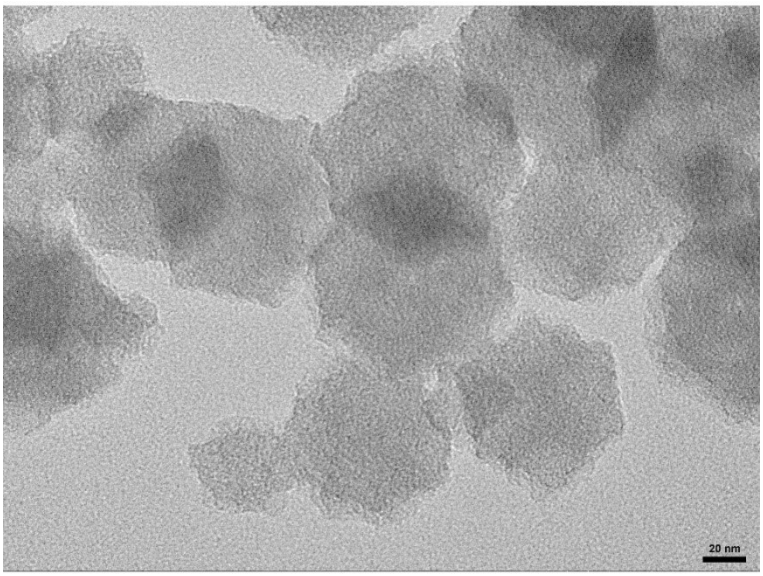

Fig. S1. TEM image of E-Z-800 with large magnification.

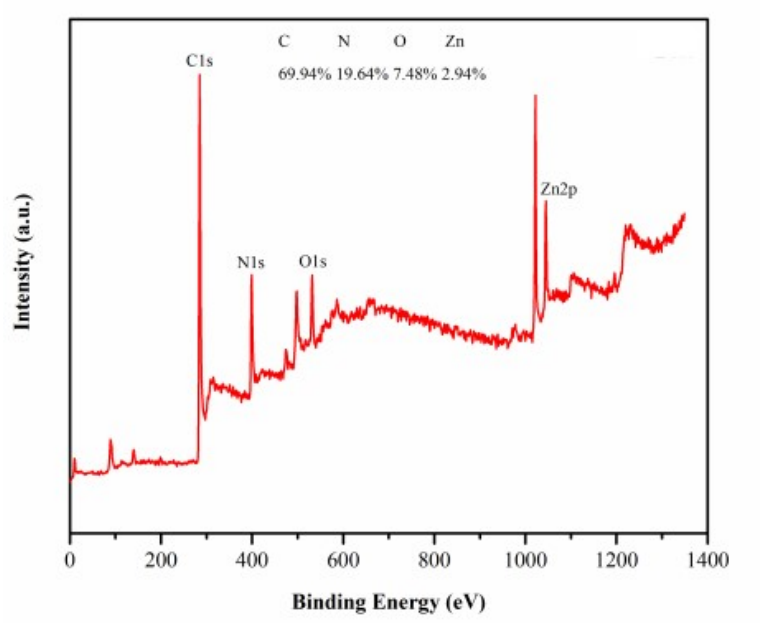

Fig. S2. XPS spectrum of E-Z-800.

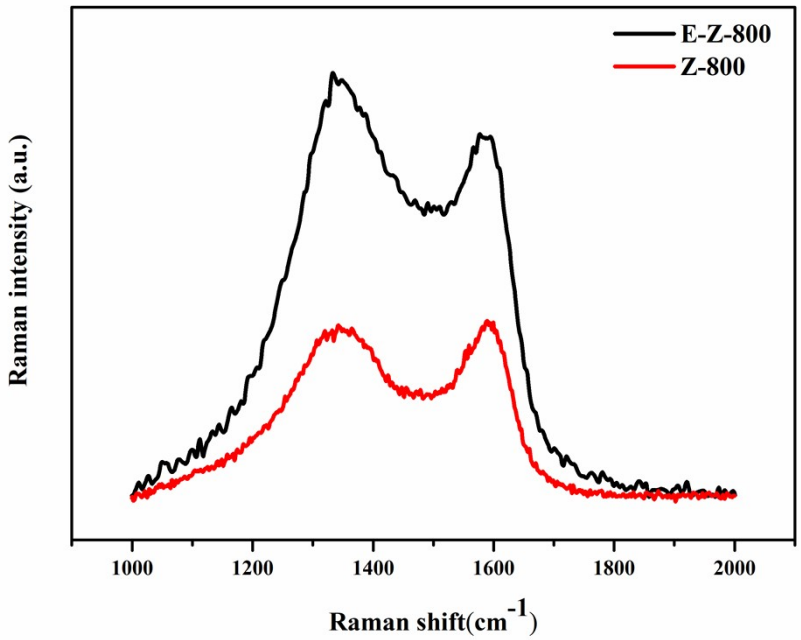

Fig. S3. Raman spectra of Z-800 and E-Z-800.

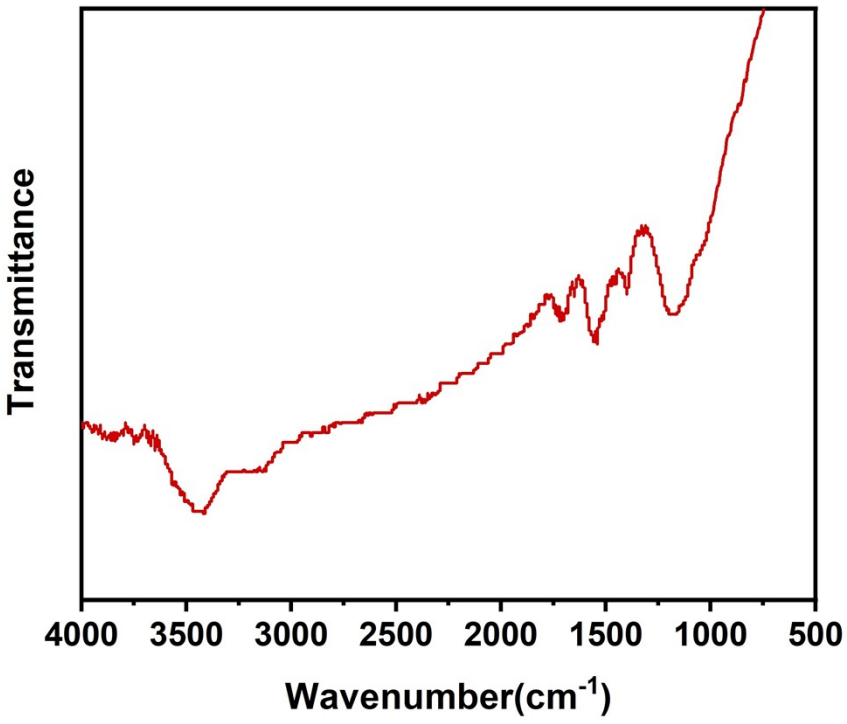

Fig. S4. FT-IR spectrum of E-Z-800.

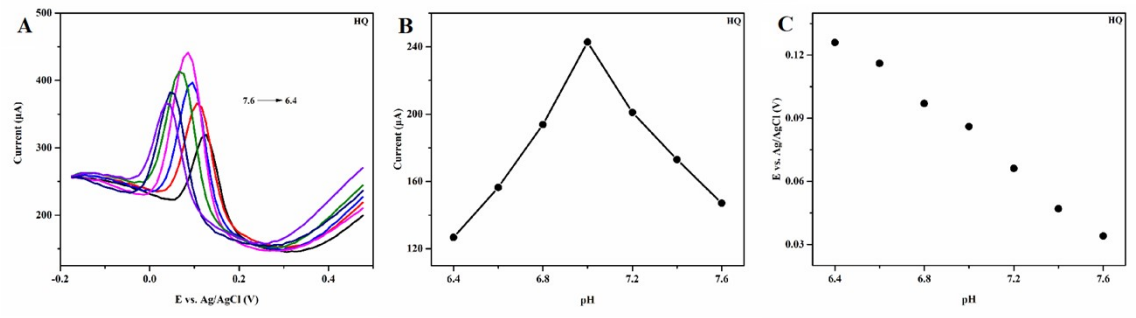

Fig. S5. (A) SWV curves of 0.1 mM HQ on E-Z-800/GCE at different pH; pH is from 6.4 to 7.6. (B) Corresponding peak currents versus pH. (C) Corresponding peak potentials versus pH.

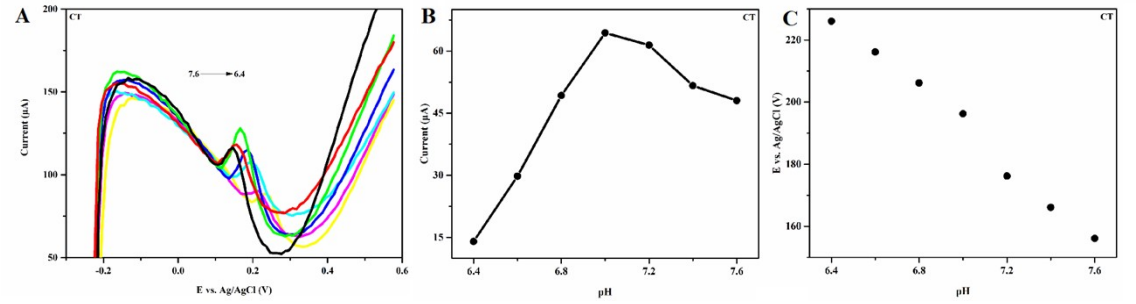

Fig. S6. (A) SWV curves of 0.1 mM CT on E-Z-800/GCE at different pH; pH is from 6.4 to 7.6. (B) Corresponding peak currents versus pH. (C) Corresponding peak potentials versus pH.

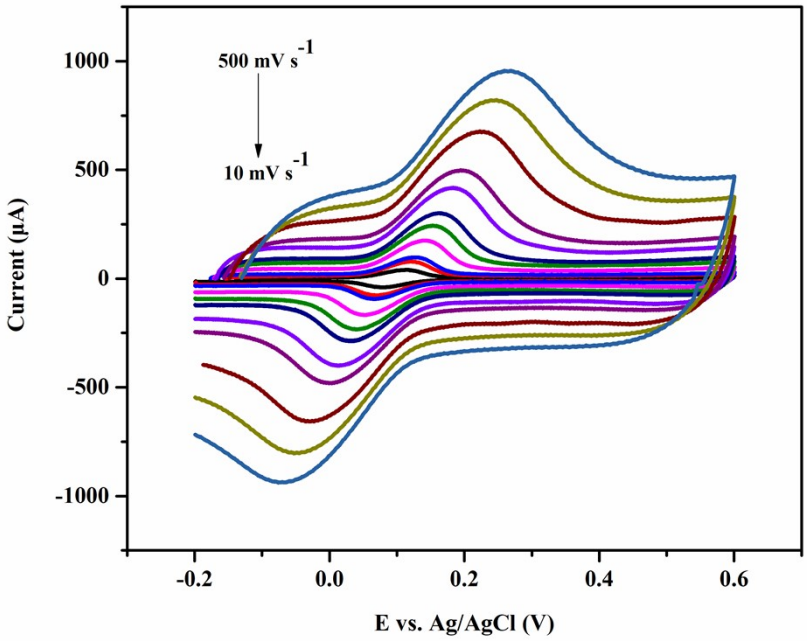

Fig. S7. CVs of 0.1 mM HQ on E-Z-800/GCE with different scan rates in 0.1 M PBS (pH 7.0) solution; Scan rates (from inner to outer) were from 10 to 500 $mV \cdot s^{-1}$.

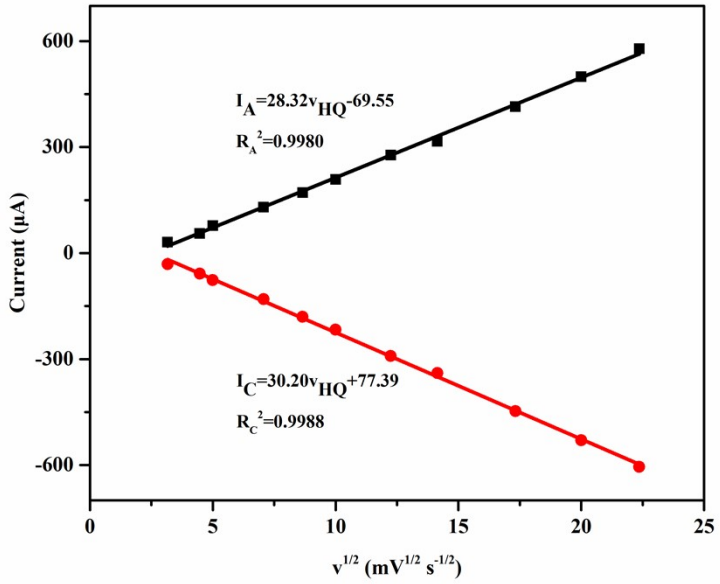

Fig. S8. The plots of redox peak currents (Ip) versus the square root of scan rate.

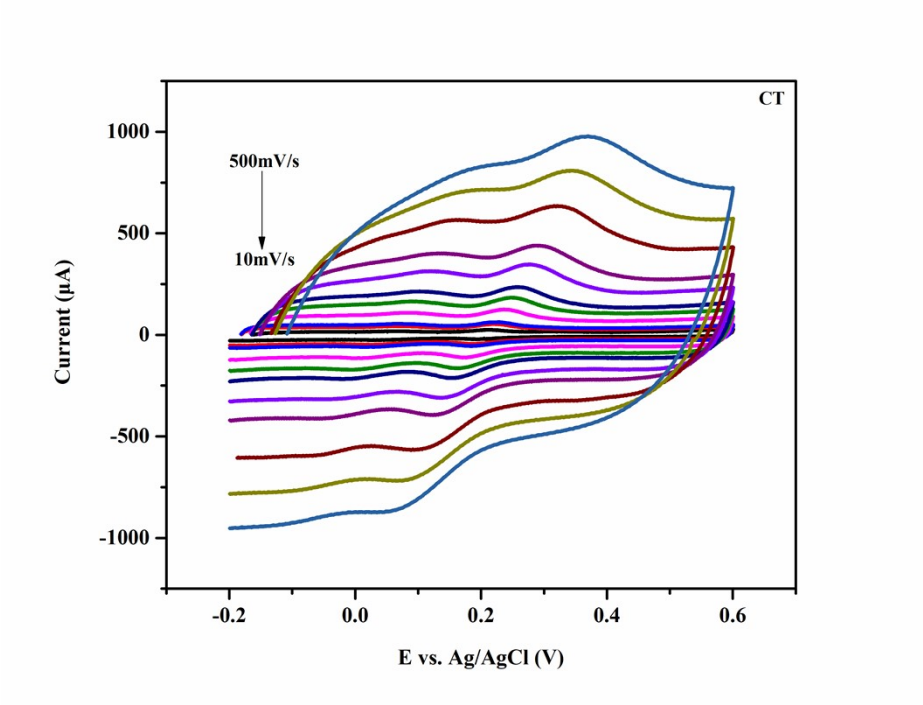

Fig. S9. CVs of 0.1 mM CT on E-Z-800/GCE with different scan rates in 0.1 M PBS (pH 7.0) solution; Scan rates (from inner to outer) were from 10 to 500 $mV \cdot s^{-1}$.

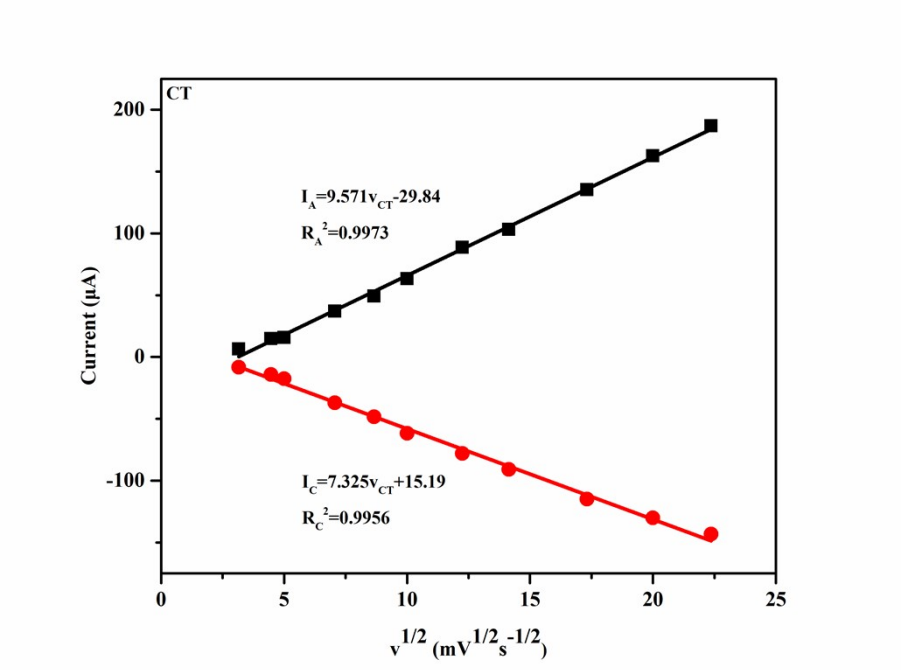

Fig. S10. The plots of redox peak currents (Ip) versus the square root of scan rate.

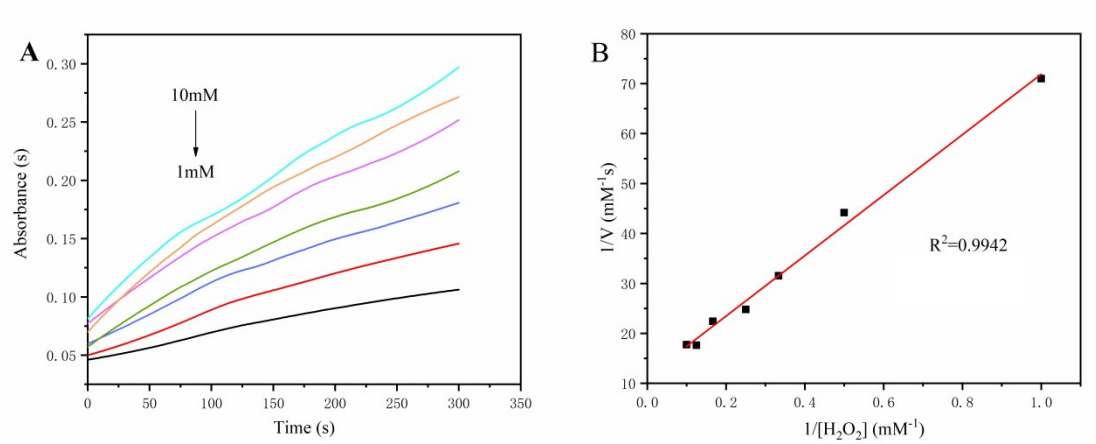

Fig. S11. (A) Time-dependent absorbance changes of TMB oxidation catalyzed by variable concentrations of H_2O_2 in the presence of E-Z-800. (B) Relation curve of the reciprocal of H_2O_2 concentration and the reciprocal of reaction rate.

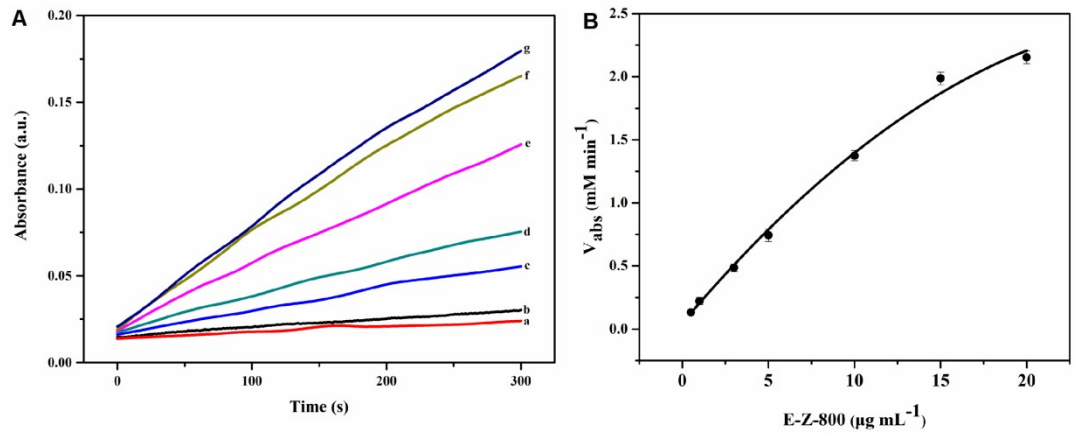

Fig. S12. (A) Time-dependent absorbance changes of TMB oxidation catalyzed by H_2O_2 in the presence of variable concentrations of E-Z-800. (B) Relation curve of the concentrations of E-Z-800 and the reaction rate.

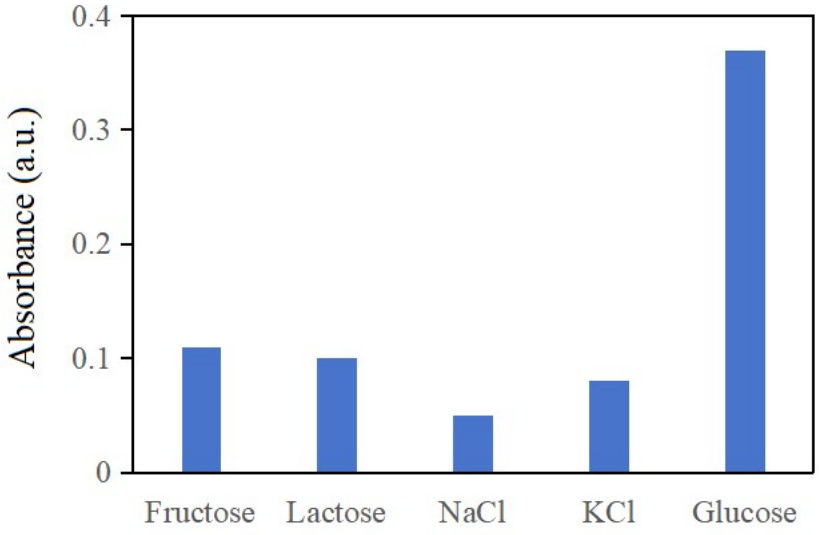

Fig. S13. Changes of absorbance signals for glucose, fructose, lactose, NaCl and KCl respectively.

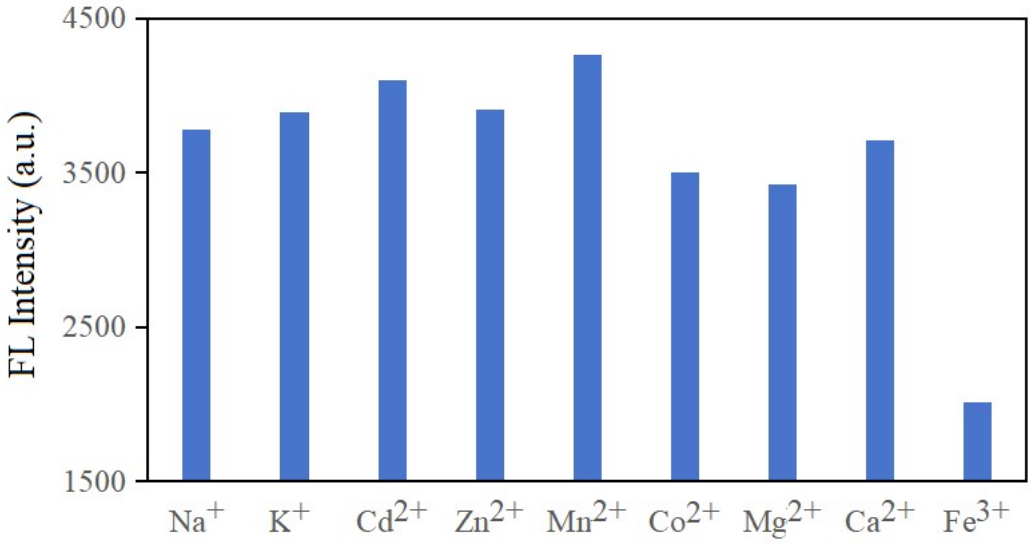

Fig. S14. Changes of FL intensities for Na^{+}, K^{+}, Cd^{2+}, Zn^{2+}, Mn^{2+}, Co^{2+}, Mg^{2+}, Ca^{2+} and Fe^{3+} respectively.